Effect of reservoir tillage on rainwater harvesting and soil erosion control under a developed rainfall simulator

Haytham M. Salem, Constantino Valero, Miguel Ángel Muñoz, María Gil-Rodríguez, Pilar Barreiro

Keywords:
Spatial rainfall distribution
Drop size
Depression form
Runoff
Sediment

A B S T R A C T

Soil erosion is a serious environmental threat in the Mediterranean region due to torrential rainfalls, and it contributes to the degradation of agricultural land. Techniques such as rainwater harvesting may improve soil water storage and increase agricultural productivity, which could result in more effective land usage. Reservoir tillage is an effective system of harvesting rainwater, but it has not been scientifically evaluated like other tillage systems. Its suitability for the conditions in Spain has not been determined. To investigate and quantify water storage from reservoir tillage and how it could be adapted to improve infiltration of harvested rainwater, a laboratory-scale rainfall simulator was developed. Rainfall characteristics, including rainfall intensity, spatial uniformity and raindrop size, confirm that natural rainfall conditions are simulated with sufficient accuracy. The simulator was auto-controlled by a solenoid valve and three pressure nozzles were used to spray water corresponding to five rainfall intensities ranging from 36 to 112 mm h^{-1} for 3 to 101-year return period with uniformity coefficients between 83 and 94%. In order to assess the reservoir tillage method under surface slopes of 0, 5, and 10%, three soil scooping devices with identical volume were used to make depressions in the following forms: a) truncated square pyramid, b) triangular prism, and c) truncated cone. These depressions were compared to a control soil surface with no depression. For the loam soil used in this study, results show that reservoir tillage was able to reduce soil erosion and surface runoff and significantly increase infiltration. There was significant difference between the depressions and the control. Compared to the control, depression (a) reduced surface runoff by about 61% and the sediment yield concentration by about 79%.

1. Introduction

Soil erosion is a major environmental threat in the Mediterranean region due to torrential rainfalls and the arid and semi-arid conditions, and it contributes to the degradation of agricultural land (Cerdà, 2002; Cerdà et al., 2009; Jordán et al., 2010; Lal, 1999). Rainwater harvesting has the potential to reduce soil erosion and improve the productivity of these areas. Rainwater harvesting is a general term used to describe the collection and concentration of runoff for many uses, including agricultural and domestic use (FAO, 1993; Oweis and Hachum, 2006). The rainwater harvesting strategy is based on discontinuities. And those discontinuities are found in nature (stones, plants, microtopography) (Kakembo et al., 2013).

"In situ" systems are the simplest and cheapest rainwater harvesting approaches and can be practiced in many farming systems. Also called soil and water conservation systems, they involve the use of methods to increase the amount of water stored in the soil profile by trapping or holding the rain where it falls (Brhane et al., 2006; Fleskens et al., 2005; Stott et al., 2001). Soil water conservation is main concern in semiarid land, and this is why harvesting rainwater is so important (Gao et al., 2013). Rainwater harvesting is being also, used by the plants and stones under natural conditions (Cerdà, 1997a,b, 2001). It may be close to the definition of micro-catchments techniques, but in any case, it becomes an alternative in arid and semi-arid regions, where precipitation is low or infrequent during the dry season, and there is a need to store the maximum amount of rainwater during the wet season for use at a later time.

Another concept related to "in situ" rainwater harvesting that involves different techniques is known as "Reservoir Tillage." This approach was developed under the consideration that tillage can provide increased levels of surface storage, and it may represent one of the most effective means of controlling both runoff and soil erosion. Reservoir tillage creates basins or pits to hold water in place, allowing it to infiltrate the soil and thus preventing runoff (Hackwell et al., 1991; Rochester et al., 1994). Soil bunds are a similar technique to reduce the connectivity of the runoff (Adimassu et al., 2013). Reservoir tillage has been defined by Patrick et al. (2007) as a system in which numerous small surface depressions are formed to hold and collect water during irrigation or rainfall to prevent surface runoff. Currently, reservoir tillage is used predominantly for soil erosion control in environments with high annual, but low intensity rainfall, such as semi-arid environments. This method has the potential to benefit semi-arid environments compared to other direct water harvesting methods, such as ridge and furrow (Kronen, 1994), because the large infiltration surface area created by the depressions and the small depth of ponded water in the shallow depressions are likely to result in higher infiltration rates and therefore less surface runoff and evaporative loss (Mrabet, 2002; Patrick et al., 2007). This is due to the fact that, when rainfall tillage is used, rainfall collects in the mini-reservoirs, allowing more time for infiltration, which in turn reduces runoff and its potential to detach and transport soil particles (Ventura et al., 2005).

For any given soil conditions, the volume of water harvested by a depression depends on the volume of the depression and its depth, which determines the maximum head of water in the depression. The volume of water further depends on the slope, which influences the reservoir capacity. Therefore, reservoir tillage under conditions of high evaporation rates and high-intensity rainfall should be adapted to maximize the volume of runoff collected without impeding water infiltration through compaction during the creation of the depressions, either by wheel traffic or by the implement itself. Patrick (2005) conducted a similar work on reservoir tillage. The project was carried out through modeling and experiments under soil bin, rainfall simulator and glasshouse environmental conditions, and the author reported that the reservoir tillage reduced surface runoff by 54% and 91% when the depressions were positioned along and across the slopes, respectively.

Rainfall simulation is an experimental method widely used to determine the relative erodibility of different soil materials and other hydrological model parameters, as well as to quantify the influence of different soil management systems, such as conservation tillage, on infiltration and runoff generation (Niebes et al., 2001). Rainfall simulators are research tools designed to apply water in a form similar to natural rainstorms. simulators permit a rapid collection of reproducible data in laboratory and field experiments (Aksoy et al., 2012; Esteves et al., 2000; Miller, 1987) and are widely used in semiarid environments where rainfall is low and soil erosion is a low frequency–high magnitude process that needs accurate measurements (Cerdà, 1999a,b).

Desirable characteristics for rainfall simulators used in erosion and hydrological studies include the rainfall intensity, spatial rainfall uniformity over the entire test plot, the drop size, its distribution and terminal velocity. Other important factors include the accurate control of rainfall intensity, the similarity to natural rainfall in terms of kinetic energy, the repeatability of the simulated rainstorms, and the improved mechanical and technical reliability for simple and easy transportation within research areas (Abudi et al., 2012; Cerdà, 1999a; Clarke and Walsh, 2007; Humphry et al., 2002; Lascano et al., 1997; Munster et al., 2006).

The main objectives of this work were: (i) to research, understand and quantify water storage from reservoir tillage and how it could be adapted to improve infiltration of harvested water for use in semi-arid environments; (ii) to determine the relationship between surface slope and water harvesting reservoir capacity; and (iii) to assess the rainwater harvesting effectiveness of different depression geometric forms under different soil slopes and different rainfall intensities.

With the aim and objectives stated for this study, specific hypotheses will be tested. Those hypotheses are: (1) to develop a laboratory-scale rainfall simulator to compare rainwater harvesting capacity, runoff and soil losses under variable rainfall intensities, (2) to achieve desirable characteristics for a rainfall simulator, include the rainfall intensity, spatial rainfall uniformity over the entire test plot, and the drop size in a form similar to natural rainstorms.

2. Materials and methods

2.1. Rainfall simulator design

A reliable, accurate rainfall simulator was needed for soil erosion studies on agricultural land. A laboratory-scale rainfall simulator was developed to compare rainwater harvesting capacity, runoff and soil losses under variable rainfall intensities. This is a tool that has been widely used for more than 50 years to evaluate hydrological parameters such as infiltration, runoff, and sediment yield because of its low cost and easy operation. It also permits data to be obtained under controlled conditions within relatively short time periods, and the results of rainfall simulation tests can be used for comparative purposes in erosion studies (Foster et al., 2000; Navas et al., 1990).

Precipitation data from the Madrid weather station (40° 24′ 43″ N lat.; 3° 40′ 41″ W long., 667 masl) were used to calibrate the rainfall simulation tests. A set of records from the 50-year time period between 1962 and 2011 was analyzed to calculate rainfall intensity. Maximum annual precipitations recorded during 30 min were converted into mm h^{-1}. According to Arnaéz et al. (2007), the data prediction was performed with a regression equation. The recurrence intervals and the exceedance probability for available data were derived according to (Blom, 1958).

The designed rainfall simulator has been settled on an A-frame steel structure of 35 mm of diameter. The legs are telescopic, which allow the height to be increased or decreased so as to keep the simulator leveled when placed on a slope for outdoor experiments. Three different axial flow full cone nozzles, Lechler (468.528.30 and 468.808.30) with spread angle of 120° and Lechler (468.726.30) with spread angle of 90° were selected for different rainfall intensities between 33 and 121 mm h^{-1}. These nozzles were fitted to a 20 mm steel pipe at the top of the structure at a height of 2.3 m with a triplet nozzle holder that eased the switching between different nozzles. This height is adequate for creating terminal velocities similar to natural rainfall for all drop sizes above the soil surface. The flow rate was auto-controlled by a solenoid valve (Bermad, 0.7–10 bar, ISO: PN 10, and 24 V AC), and the pressure was monitored by two glycerin manometers. RS pressure transmitter (348–8188) 4–20 mA analog output, and pressure regulator installed in the supplying pipe of the simulator.

A National Instruments LabVIEW® programming tool was used for building an application that consists of a customized user interface, a display interface for pressure monitoring and an on/off valve. The block diagram contains a graphical representation of the code consisting of functions to read from inputs, write to outputs and make calculations and decisions. The inputs and outputs (pressure transmitter and solenoid valve) were connected to a Data Acquisition Board (DAQB; National Instruments 6008 USB). The front panel is the user interface, which has controls for selecting the time flow and monitoring the pressure.

2.2. Rainfall simulator calibration

2.2.1. Spatial rainfall distribution

An experiment was carried out on the rainfall produced by the rainfall simulator in order to characterize its spatial rainfall distribution. The experiment aimed to get information about the homogeneity or heterogeneity of the rainfall and to determine the maximum area at which a homogeneous distribution of rainfall could be obtained. Twenty rain gauges (82 mm diameter) were placed on a 60 cm × 80 cm by 20 cm × 20 cm grid. Rain was collected in the gauges for 10 min of continuous flow from the simulator, and the volumes in each gauge were measured using a graduated cylinder in (ml) and then converted into intensity values (mm h^{-1}). The Coefficient of Variation (CV) and the mean Christiansen Uniformity (CU) coefficient (Christiansen, 1942) were calculated using Eq. (1).

$$\mathrm{CU} = 100\% \left(\frac{1 - \sum_{i=1}^{n} |x_i - \bar{x}|}{\bar{x} * n} \right) \tag{1}$$

where each expression stands for:

$1 - \sum_{i=1}^{n} |x_{i-\bar{x}}|$ Sum of the absolute deviations from average water quantity for all rain gauges (ml).

x_i water quantity per rain gauge (ml).
$\bar{x}$ arithmetic mean of applied water amount per rain gauge (ml).
n total number of rain gauges.

The spatial distribution of rainfall was described by using Sigmaplot 11.0 software.

2.2.2. Drop size distribution

For the analysis of drop size distribution, Indication Paper (water-sensitive paper/card), first introduced and described by Wiesner (1895) and Hall (1970). This method is based on the assumption that a drop falling upon a uniform absorbent surface produces blue spots with a diameter proportional to the diameter of the drop. Water-sensitive paper can be considered the most frequently used method for measuring the drop size distribution of natural or simulated rainfall (Erpul et al., 1998; Ries et al., 2009). Moreover, it has been widely used in semi-arid environments under natural (Cerdà, 1997a,b) and simulated rainfall (Cerdà et al., 1997).

To determine the artificial rainfall drop size distribution, fifty cards (52 mm × 76 mm) were exposed to simulated rainfall for two seconds under different rainfall intensities. All of these cards were photographed with an RGB camera (Sony Alpha 77. 24 Mpix). In order to calculate the median drop size (D_{50}) which is defined as the drop size where 50% of drops generated in the storm are larger and 50% is smaller. D_{50} (mm) was estimated using Matlab 7.0 software on the images.

2.3. Preparation of experimental units

The soil used in this study was collected from an *Ap horizon* (0–30 cm). The soil, classified as Vertic Luvisol (FAO, 1988), was collected from the experimental field "El Encín" which is located in Alcalá de Henares, Madrid (40°29′N lat.; 3°22′W long.). A winter/spring cereal and leguminous plant crop rotation is carried out annually in this soil. The area's physical and chemical characteristics (Table 1) indicate a loamy soil with a low organic content. The experiments took place in the Rural Engineering Department of the Technical University of Madrid. A reinforced plastic tray with a thickness of 10 mm and internal dimensions of 78 cm length, 58 cm width and 30 cm depth was used. A steel sieve with holes 2 mm in diameter was fixed at a height 5 cm from the tray's ground surface to provide a drainage area under the soil sample. An aperture on the tray frame at the bottom of the sieve allowed for the free infiltration of soil moisture.

Table 1
Soil characteristics.

Coarse skeleton (>2 mm) (%, g g^{-1})	1
Sand (g kg^{-1})	390
Silt (g kg^{-1})	400
Clay (g kg^{-1})	210
Textural class	Loam
Organic matter (g kg^{-1})	15
Carbon (g kg^{-1})	5.7

A transparent plastic collector was set at the bottom of the tray slope to act as a free draining lower boundary (seepage face) and to collect surface runoff in bottles. The soil was gently crushed before passing through a 6 mm sieve, and the sieved soil was thoroughly mixed to minimize the difference among treatments. In each tray, the 22 cm thick soil was packed in two 11 cm layers to achieve a 1.25 g cm^{-3} bulk density. The volumetric soil moisture content varied between 17 and 19%, as measured by the SM300 Soil Moisture Sensor for all experiments.

2.3.1. Selected depression forming tools

The depressions (mini-reservoirs) were created by manually scooping the soil with a small amount of pressure. Hand-operated scoops were manufactured from reinforced plastic with the same volume (1 l) and depth (12 cm). To determine the proper shape for increasing rainwater harvesting (Fig. 1), the scoops were designed in the following three shapes: a) truncated square pyramid, b) triangular prism, and c) truncated cone.

In the experiments, the shapes were inserted into the soil to create rows of depressions. The depressions were spaced at 14 cm, and a distance of 12 cm was left between each row.

Fig. 2, shows the surface depressions for the four soil treatments (reservoir tillage treatments) using shape (a) in surface (1), shape (b) in surface (2), and shape (c) in surface (3), while surface (4) has no depressions (control). After all the treatments were created, the tray was put on a hydraulic trolley under the rainfall simulator, and five different rainfall intensities were simulated for 30 min: 36.7, 58.8, 81.4, 97.8, and 112.6 mm h^{-1} For each factorial combination of soil treatment and rainfall intensity, three slope angles were used: 0°, 5° and 10°. The slope angles of 5° and 10° were created by sliding square tubes of 7 cm and 14 cm in length, respectively. This resulted in 60 randomized treatments, and each was replicated three times. Because of the difference in the ratio of depression surface area to total catchment surface area between the depressions and the control, a slight correction was made to scale down the volume of runoff recorded in the depression experiments, as to make data from both experiments directly comparable. Runoff and sediment samples were collected in small bottles at 3 min intervals during each simulated rainfall event from the moment the runoff started to flow until it ceased.

The data obtained from each treatment included the mean runoff (mm h^{-1}), the runoff coefficient (the percentage of rainfall that becomes runoff), and the time lag (the number of seconds between the beginning of the rainfall simulation and the beginning of the runoff). Sediment was deposited, separated from the water, dried in an oven to a constant weight at 105 °C for 24 h, and weighed. The sediment concentration was defined as the ratio of dry sediment mass to runoff volume, while the sediment yield rate was determined by dividing the sediment yield per unit area for the recorded period of time. Infiltration rates were determined by subtracting the measured runoff rates from the rainfall application rate. Thus, evaporation, interception and surface storage components (water harvesting reservoir capacity) were considered as infiltration.

Data were analyzed by the General Linear Model of ANOVA. The SPSS Statistic 17.0 was used to test for significant differences and least significant difference (LSD) between the treatments.

3. Results and discussion

3.1. Spatial rainfall distribution

The rainfall simulator provided rainfall intensities between 33 and 121 mm h^{-1}, obtained from different water pressures that ranged from 0.7 to 1.5 bar using three different nozzles. The spatial rainfall distribution shows a concentric pattern with the highest rainfall amount (ml) recorded in the center and the lowest rainfall amount recorded

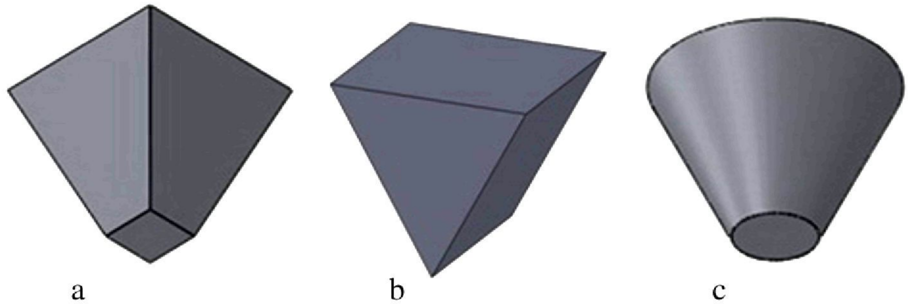

Fig. 1. Different hand-operated scoops used to form depressions.

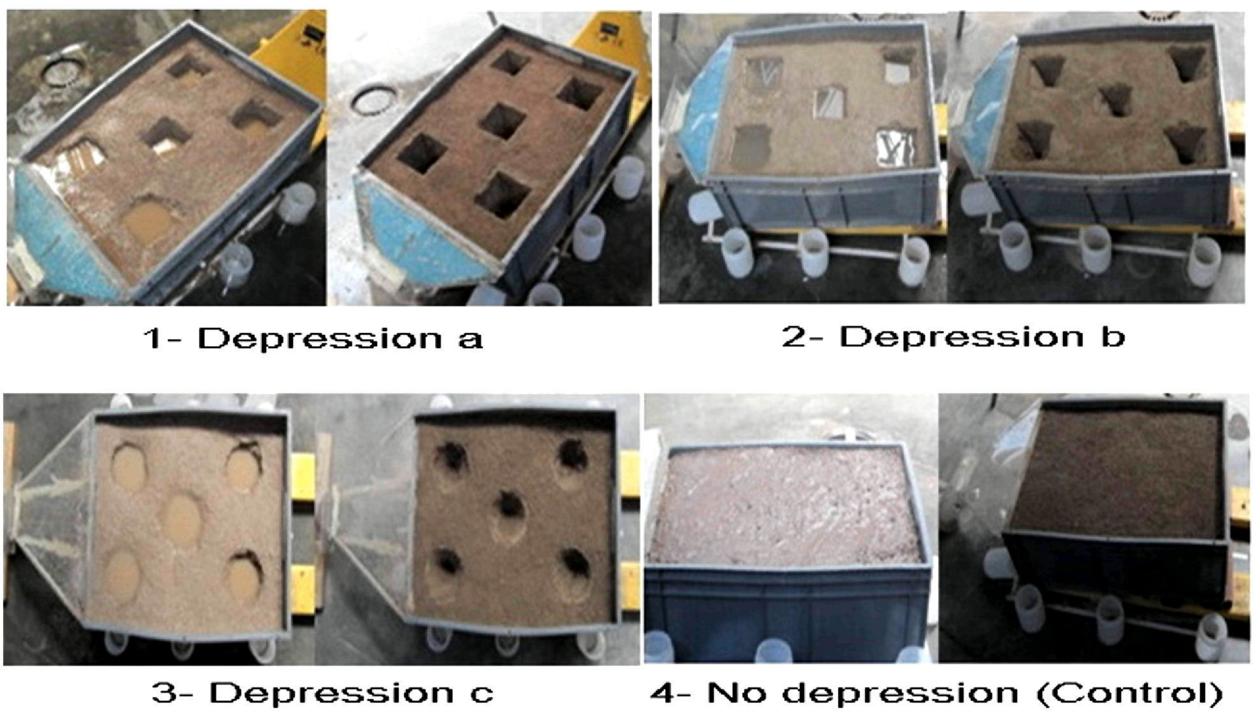

Fig. 2. Treatments with depressions using shapes (a, b, and c) compared to control treatment, before and after rainfall simulation.

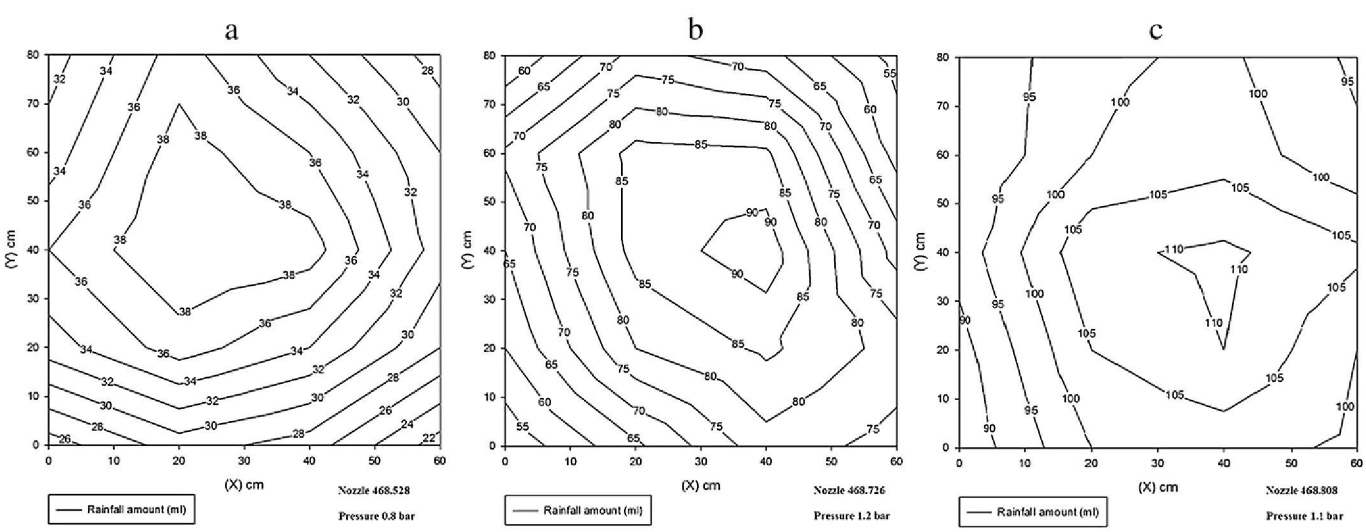

Fig. 3. (a, b, c). Distribution of simulated rainfall intensities over 60 × 80 cm plot area using (a) nozzle 468.528, pressure 0.8 bar, (b) nozzle 468.726, pressure 1.2 bar, and (c) nozzle 468.808, pressure 1.1 bar.

Table 2
Rainfall intensities and recurrence periods and coefficients of uniformity and variation for different nozzles working at different pressures over a 60 cm × 80 cm surface.

Nozzle type	Pressure (bar)	Mean rainfall intensity (mm h^{-1})	Recurrence[a] (years)	CU (%)	CV (%)
468.528	0.75	33.4	2.6	84.9	18.4
468.528	0.8	36.7	3.0	87.1	15.8
468.528	1.3	48	5.1	83	19.9
468.528	1.5	58.8	8.4	85.5	18.2
468.726	1.2	81.4	23.9	85.5	17.6
468.726	1.3	87.9	32.3	86.4	16.5
468.808	1	97.8	51.1	90.9	10.9
468.808	1.050	109.8	89.1	92.1	9.7
468.808	1.1	112.6	101.5	94.2	7.8
468.808	1.150	121.5	153.3	93.2	8.5

[a] Data obtained by the equation: $R = \exp((I_p - 12.909) / 21.579)$, $r^2 = 0.99$, where R is the recurrence period (years) and I_p is the rainfall intensity (mm h^{-1}) (Arnaéz et al., 2007).

around the rim of the plot (Fig. 3a, b, c). This deviation from maximum to minimum rainfall amount is caused by the physical properties of the nozzle and the applied water pressure. In order to create the largest possible drop size, the water pressure system was reduced as much as possible, causing a decrease in the nozzle's spray effect and creating a higher heterogeneity of spatial rainfall distribution across the plot. Otherwise, the heterogeneity decreased with increasing rainfall intensities. The major reason for accepting this drawback is that the drop size of simulated drops closely resembled natural drops, additionally, the good reproducibility of the spatial rainfall distribution and the good Christiansen Coefficient between 83 and 94% on a plot 60 × 80 cm (Table 2). This uniformity was in an acceptable range according to Esteves et al. (2000) and Pérez-Latorre et al. (2010) for rainfall simulators with plot sizes below 1 m^2.

The return periods (recurrence periods) of these rainfall intensities were calculated from Madrid weather station data and the fit curve equation came from the methods described by Blom (1958) and Arnaéz et al. (2007) (Table 2).

3.2. Drop size distribution

Drop size increased with rainfall intensity. The median drop size (D_{50}) ranged from 0.8 to 2.1 mm. It was 0.8 mm for simulated storms of 33.4 mm h^{-1}, whereas for intensities of 58.8 and 121.5 mm h^{-1}, the diameter reached 1 and 2.1 mm, respectively. These sizes are slightly smaller than those calculated by Martínez-Mena et al. (2001) and Pérez-Latorre et al. (2010). This range is narrower than that obtained by Miller (1987) with drops between 1.75 and 2.75 mm. The drop diameter of natural rainfall in western Spain is usually smaller than 2 mm (Cerdà, 1997a,b), and that observed in the experimental site ranged from 0.5 to 2 mm.

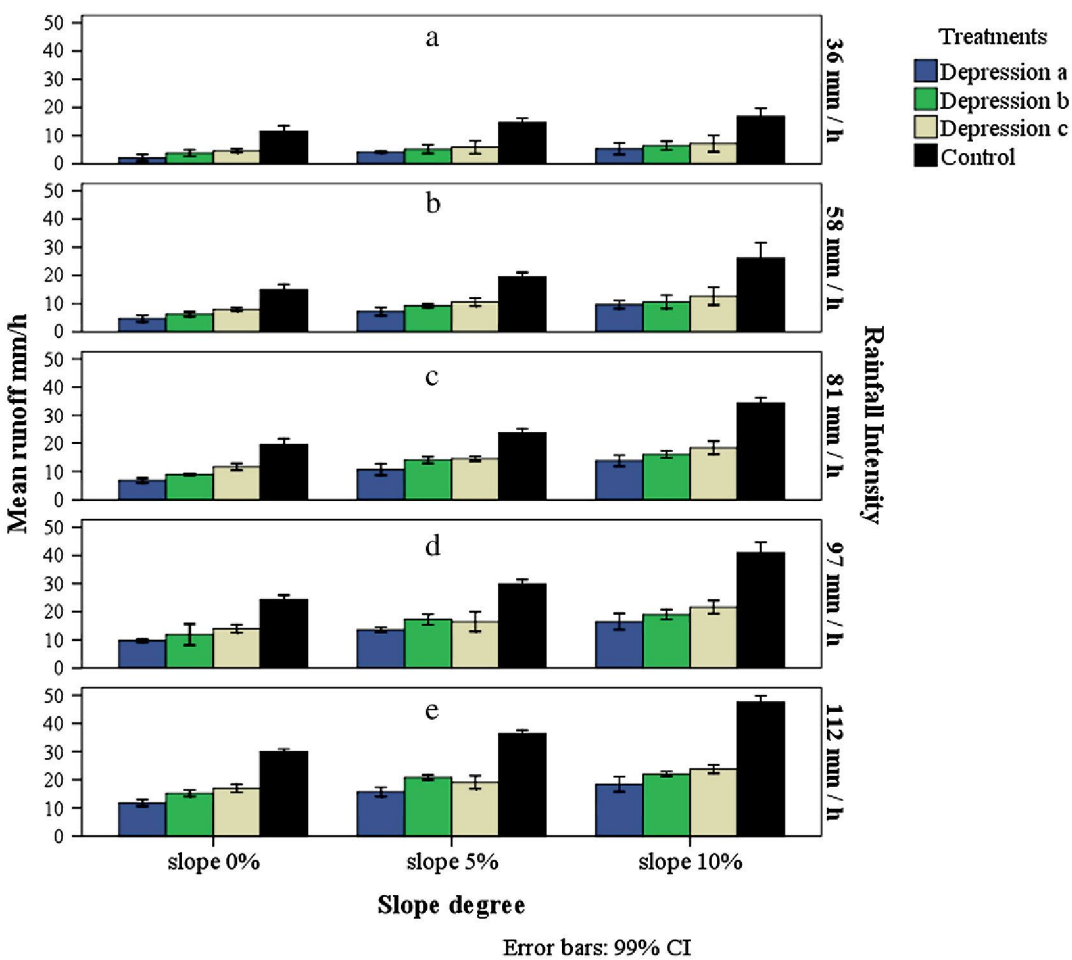

Fig. 4. Mean surface runoff of the different depression forms compared to control under different surface slope degrees and different rainfall intensities (a, b, c, d, and e) for intensities (36, 58, 81, 97, and 112 mm h^{-1}), respectively.

Table 3
Total mean of surface runoff, sediment concentration, and sediment yield rate of the different depression forms and reductions in these parameters as compared to no depression (control).

Treatments	Surface runoff ($mm\ h^{-1}$)	Sediment concentration ($g\ l^{-1}$)	Sediment yield rate ($g\ m^{-2}\ h^{-1}$)	Reduction(%)		
				Surface runoff	Sediment concentration	Sediment yield rate
Control	26.004 a	4.992 a	119.810 a	–	–	–
Depression c	13.704 b	4.267 b	57.862 b	47.30	14.52	51.71
Depression b	12.473 c	3.826 c	47.291 c	52.03	23.35	60.53
Depression a	10.036 d	2.276 d	24.065 d	61.41	54.41	79.91

The total means within a column followed by dissimilar letter are significantly different at $\alpha = 0.01$ level using the least significant difference (LSD) method.

3.3. Effect of rainfall intensity, slope and different depression forms on surface runoff and infiltration rates

Infiltration and runoff are important processes for dry-land farming in semi-arid areas. Insufficient soil moisture is one, if not the major, limiting factor for crop production in any country. Thus, any tillage system which shows a high degree of infiltration and a runoff reduction will be examined with great interest.

The surface runoff increased with rainfall intensity and surface slope. This is illustrated in Fig. 4, which shows the rate of runoff obtained as a function of slope for different rainfall intensities. For surface depressions (a, b, and c), there were significant reductions in recorded runoff rates at different rainfall intensities, as compared to a surface with no depressions (control), (Fig. 4). The total mean of surface runoff in depression treatments ranged from 10 to 13.7 mm h^{-1}. Depression treatments reduced runoff rates by about 47 to 61% compared to control treatment. Furthermore, the difference between the surface runoff in different depression forms was significant, but surface runoff was consistently lower in depression (a) as compared to the other forms (Table 3). This is due to the fact that both depressions (b and c) began to collapse with time, especially as a result of high rainfall intensities and downward slopes. On the other hand, depression (a) intercepted runoff, conserved its shape and resisted collapsing with time.

The magnitude of this difference in runoff rates between depression (a) and depression (b and c) increased with rainfall intensity and with surface slope (the total means of reductions ranged from 20 to 27%), respectively.

Fig. 5(a, b) shows the temporal evolution of runoff under different rainfall intensities for depression (a) and the control treatment with a surface slope of 10%. The response of the overland flow was faster for storms of high intensity: with simulations of 112 mm h^{-1}, the runoff began at 110 and 88 s under depression (a) and control treatment, respectively. For storms with a low intensity of 36 mm h^{-1}, on the other hand, surface runoff started 580 and 274 s after the beginning of the simulated rainfall, under depression (a) and control treatment, respectively. Additionally, the runoff coefficient ranged from 14.5 to 19.6% for depression (a), while for the control treatment, it ranged from 41.8 to 45.9%. The runoff coefficient significantly increased with the increasing of the surface slope (Tables 4 and 5). The curves in Fig. 5(a, b) show a rapid rise of runoff during the first minutes, especially in the experiment with the highest intensity precipitation. Thereafter, runoff remained at a steady state as a result of the saturation and sealing of the soil. The depression treatments had greater steady runoff rates than the control treatment. This may be due to the fact that the time delay in runoff initiation represents the depression benefits in enhancing infiltration during the first stages of rain.

The volume of harvested precipitation decreased with surface slope but increased with rainfall intensity. This is illustrated in Fig. 6, which shows the infiltration rate obtained as a function of slope for different rainfall intensities. There were significant differences between all treatments, especially between the depression treatments and the control (e.g., for low rainfall intensity 36 mm h^{-1} and slope 10%, the infiltration rate of depression (a) increased by 37%, compared to the control treatment). This may be due to the large infiltration surface area created by depressions. Further, the geometric shape of depression (a) enhanced the lateral and longitudinal infiltration into the soil during the first minutes of the rainfall simulation.

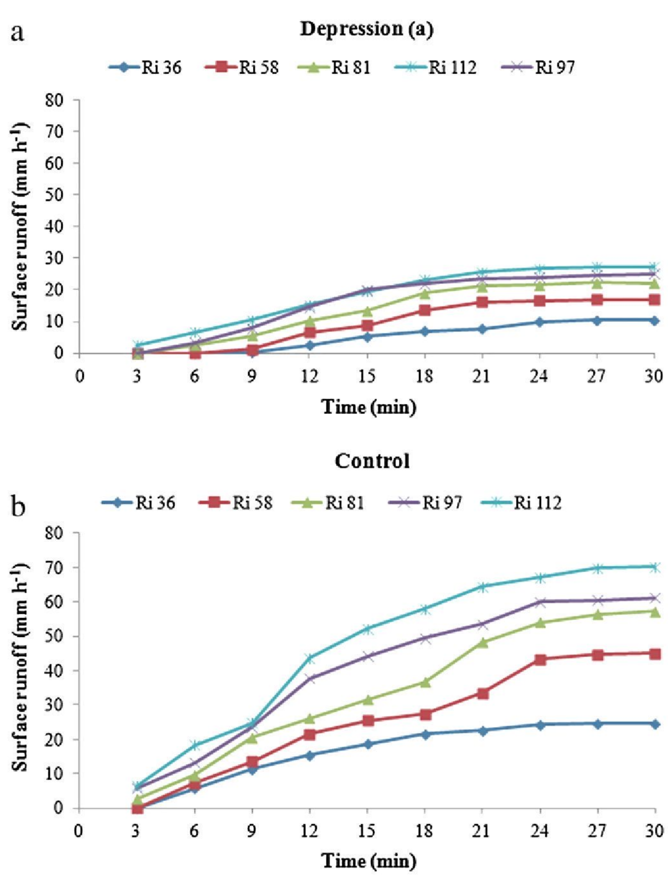

Fig. 5. (a, b). Surface runoff as a function of time of different rainfall intensities (Ri), for depression (a), and no depression (control) under slope of 10%, respectively.

Table 4
Total mean of infiltration rate, time lag, and runoff coefficient of the different depression forms compared to control.

Treatments	Infiltration rate ($mm\ h^{-1}$)	Time lag (s)	Runoff coefficient (%)
Control	50.9 d	228 d	34.2 a
Depression (c)	63.3 c	371 c	17.5 b
Depression (b)	64.5 b	384 b	15.7 c
Depression (a)	66.9 a	426 a	12.6 d

The total means within a column followed by dissimilar letter are significantly different at $\alpha = 0.01$ level using the least significant difference (LSD) method.

Table 5
Mean time lag and runoff coefficient with stander errors of depression (a) and no depression (control) under surface slope 0 and 10%, with different rainfall intensities.

Rainfall intensity (mm h^{-1})	Time lag (s)[a]				Runoff coefficient (%)[a]			
	Depression (a)		Control		Depression (a)		Control	
	Slope				Slope			
	0%	10%	0%	10%	0%	10%	0%	10%
36	920 ± 50.5	580 ± 5	449 ± 9.7	274 ± 6.2	5.9 ± 0.3	14.5 ± 0.6	31.2 ± 0.6	45.9 ± 0.8
58	657 ± 4.6	471 ± 5.6	308 ± 3.5	251 ± 10.4	8 ± 0.2	16.5 ± 0.2	25.5 ± 0.4	44.5 ± 0.9
81	488 ± 7.3	287 ± 6.1	290 ± 7.6	132 ± 5.4	8.4 ± 0.1	16.9 ± 0.2	23.8 ± 0.3	42.1 ± 0.3
97	124 ± 15.6	259 ± 8.2	273 ± 4.6	96 ± 8.7	10 ± 0.1	16.9 ± 0.3	24.9 ± 0.2	41.8 ± 0.4
112	125 ± 9.5	110 ± 5.5	244 ± 7	88 ± 7.6	10.5 ± 0.1	16.4 ± 0.2	26.5 ± 0.1	42.2 ± 0.2

[a] ± at 99% confidence interval.

3.4. Erosive response

As a direct response to the runoff produced, soil erosion was also consistently lower in the depression treatments as compared to the control. This is illustrated in Fig. 7, which shows the sediment yield rate obtained as a function of slope for different rainfall intensities. There were significant differences between all treatments; in general, depression treatments reduce the total sediment yield rate by about 51 to 79% compared to the control treatment (Table 3). Also, there were significant differences between depression forms, and the magnitude of this difference in sediment yield between depression (a) and depressions (b and c) increased with rainfall intensity and with surface slope (the total means of reductions ranged from 49 to 58%). This behavior has also been found in Fig. 8, which shows the sediment yield rate as a function of time in depression (a)'s treatment and control for different rainfall intensities at a surface slope of 10%. The sediment yield rate increased significantly with the increasing of rainfall intensity and with surface slope, but this increase was notable lower in depression (a) compared to the control treatments. This reduction in the amount of sediment yield rate is a result of having a geometrically ordered soil surface roughness created with the depressions, which reduces the runoff rate and velocity. Soil surface roughness is an important factor in preventing soil erosion (Eltz and Norton, 1997).

The curves of suspended sediment concentration for depression (a)'s treatment at the surface slope of 5% with different intensities are illustrated in Fig. 9. The highest sediment concentration is recorded

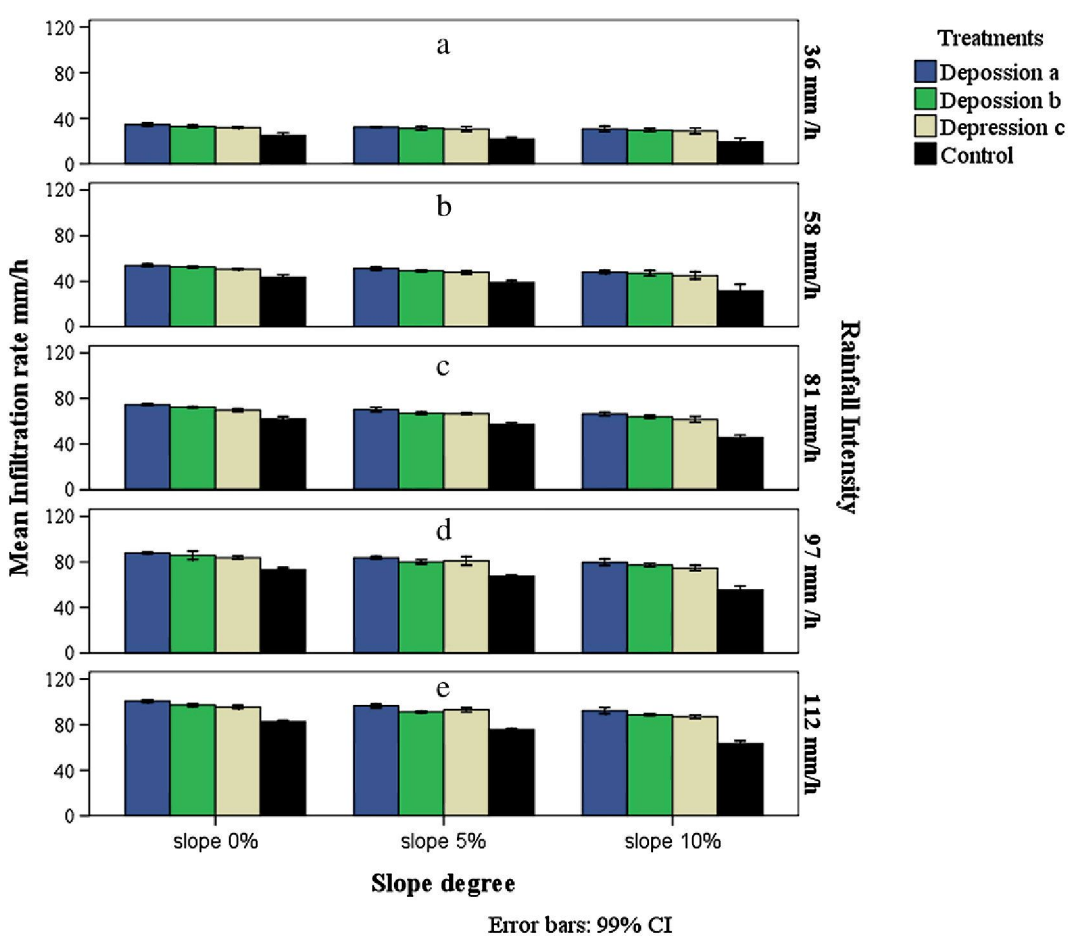

Fig. 6. Mean infiltration rate of the different depression forms compared to control, under different surface slope degrees and rainfall intensities (a, b, c, d, and e) for intensities (36, 58, 81, 97, and 112 mm h^{-1}), respectively.

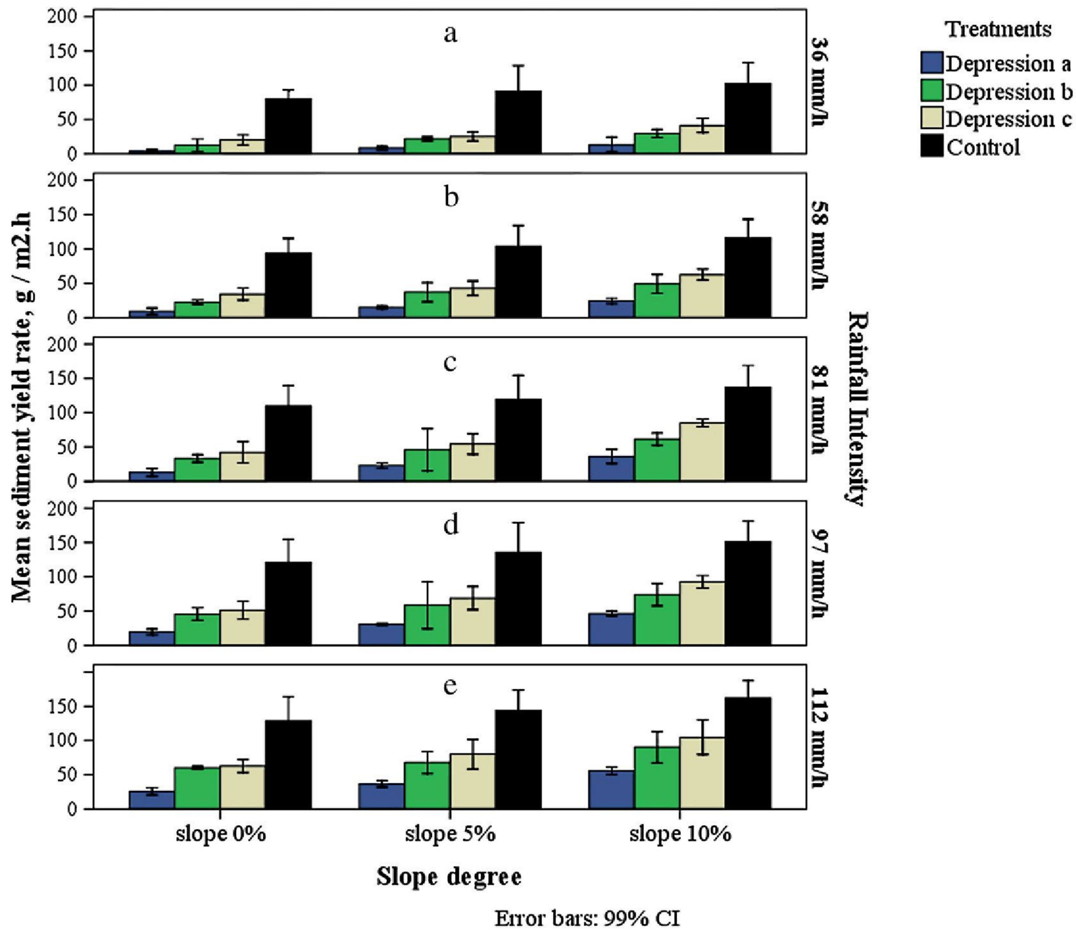

Fig. 7. Mean sediment yield rate of the different depression forms compared to control, under different surface slope degrees and rainfall intensities (a, b, c, d, and e) for intensities (36, 58, 81, 97, and 112 mm h^{-1}), respectively.

at the beginning of the experiments, especially with rainfall intensities of 81 and 97 mm h^{-1}. Thereafter, the erosive response quickly decreases with time. This response is related to the sediment availability on the soil surface between depressions in the first minutes. As the simulation progresses, the sediment output diminishes due to the exhaustion of available particles and to the protective effect of the depression against the detachment and transportation of soil particles.

Sediment concentration processes were significantly different between the depression treatments and the control treatment (e.g., depression (a) decreased the total sediment concentration by 54% compare to soil with no depressions and by 40 and 46% compare to depression (b and c), respectively) (Table 3).

This is explained by the fact that, when the reservoir tillage was used, rainfall collected in the depressions (mini-reservoirs), allowing more time for infiltration, which reduced runoff and its potential to detach and transport soil particles. Detachment and transport by the concentrated flow is one of the main processes involved in soil erosion (Foster and Meyer, 1975).

4. Conclusions

Reservoir tillage is an old system of harvesting water, but it has not been evaluated scientifically like other tillage systems. It was considered an effective method of harvesting water under high-intensity rainfall of short duration common in semi-arid areas. To research and quantify water storage from reservoir tillage and how it could be adapted to improve infiltration of harvested rainwater, an auto-controlled laboratory rainfall simulator that could obtain variable rainfall intensities with drop sizes similar to natural rain was developed.

The rainfall simulator was constructed using different three full cone nozzles and was auto-controlled by a solenoid valve. The simulator provided realistic rainfall intensities (between 33 and 121 mm h^{-1}) and drop sizes (from 0.8 to 2.1 mm), for runoff experiments, with uniformities ranging between 83 and 94%.

Three different soil surface depression formations were compared to a control treatment with no depression. The experiments were conducted under the rainfall simulator for five different rainfall intensities and three surface slope degrees. There were significant differences between depressions treatments and the control; depression (a) reduced surface runoff and the sediment yield concentration by about 61 and 79%, respectively, compared to the control treatment. For reservoir tillage, a depression in the form of a truncated square pyramid (depression (a)) was considered the most appropriate depression shape, due to its potential to reduce surface runoff and to enhance the rainwater harvesting capacity, especially under high intensity rainfall and with high soil surface slopes. As a direct response to these processes, soil erosion was also consistently lower.

Reservoir tillage system can function in Spain, but lack of sufficient information about it makes its adoption suspicious. Therefore, it is necessary to continue field trials to evaluate the use of a modified seeder machine with a reservoir tillage system in the production of wheat and barley under rainfed agriculture conditions.

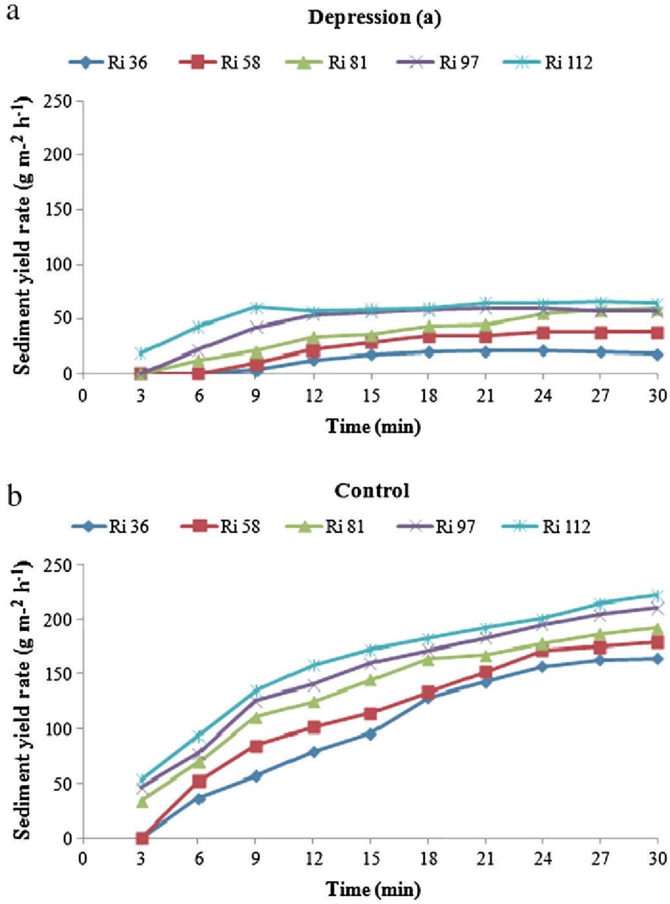

Fig. 8. (a, b). Sediment yield rate as a function of time of different intensities (Ri: Rainfall intensity, mm h^{-1}), for depression (a), and no depression (control) under slope 10%, respectively.

Acknowledgments

This study was supported and funded by the Rural Engineering Department, Polytechnic University of Madrid, and partially with the European research project "RHEA", FP7, NMP-CP-IP 245986-2. The authors would like to thank the technical workshop staff for their support. The authors would like to thank also to the Egyptian Ministry of Agriculture for the grant of Mr. Salem.

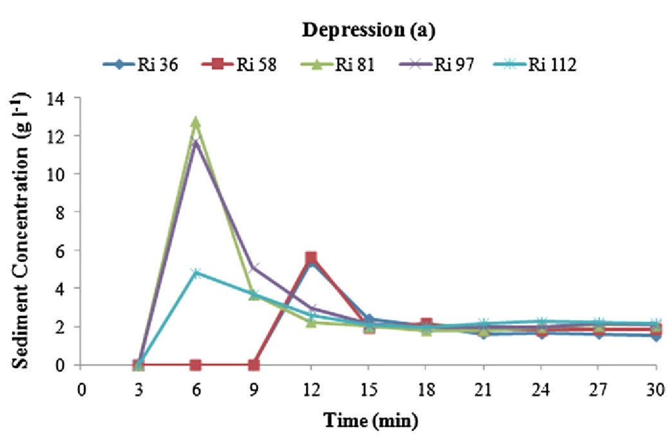

Fig. 9. Suspended sediment concentration during simulations with different intensities (Ri: Rainfall intensity, mm h^{-1}) in depression (a) treatment under surface slope 5%.

References

Abudi, I., Carmi, G., Berliner, P., 2012. Rainfall simulator for field runoff studies. J. Hydrol. 454–455, 76–81.

Adimassu, Z., Mekonnen, K., Yirga, C., Kessler, A., 2013. Effect of soil bunds on runoff, soil and nutrient losses, and crop yield in the central highlands of Ethiopia. Land Degrad. Dev. http://dx.doi.org/10.1002/ldr.2182.

Aksoy, H., Unal, N.E., Cokgor, S., Gedikli, A., Yoon, G., Koca, K., Inci, S.B., Eris, E., 2012. A rainfall simulator for laboratory-scale assessment of rainfall–runoff–sediment transport processes over a two-dimensional flume. Catena 98, 63–72.

Arnaéz, J., Lasanta, T., Ruiz-Flanoñ, P., Ortigosa, L., 2007. Factors affecting runoff and erosion under simulated rainfall in Mediterranean vineyards. Soil Tillage Res. 93, 324–334.

Blom, G., 1958. Statistical Estimates and Transformed Beta Variables. John Wiley, New York.

Brhane, G., Wortmann, C.S., Mamo, M., Gebrekidan, H., Belay, A., 2006. Micro basin tillage for grain sorghum production in semiarid areas of northern Ethiopia. Agron. J. 98, 124–128.

Cerdà, A., 1997a. Rainfall drop size distribution in Western Mediterranean Basin, València, Spain. Catena 31, 23–38.

Cerdà, A., 1997b. The effect of patchy distribution of *Stipa tenacissima* L. on runoff and erosion. J. Arid. Environ. 36, 37–51.

Cerdà, A., 1999a. Parent material and vegetation affect soil erosion in eastern Spain. Soil Sci. Soc. Am. J. 63, 362–368.

Cerdà, A., 1999b. Simuladores de lluvia y su aplicación a la Geomorfología. Estado de la cuestión Cuadernos de investigación geográfica (ISSN: 0211-6820) 25, 45–84.

Cerdà, A., 2001. Effects of rock fragment on soil infiltration, inter-rill runoff and erosion. Eur. J. Soil Sci. 52 (1), 1–10.

Cerdà, A., 2002. Agricultura y Erosión en España. Mitos y realidades. Saitabi 51–52, 473–501.

Cerdà, A., Ibáñez, S., Calvo, A., 1997. Design and operation of a small and portable rainfall simulator for rugged terrain. Soil Technol. 11 (2), 161–168.

Cerdà, A., Flanagan, D.C., le Bissonnais, Y. y, Boardman, J., 2009. Soil erosion and agriculture. Soil Tillage Res. 107–108. http://dx.doi.org/10.1016/j.still.2009.10.006.

Christiansen, J.E., 1942. Irrigation by sprinkling. Univ. Calif. Agric. Exp. Stn. Bull. 670.

Clarke, M.A., Walsh, R.P.D., 2007. A portable rainfall simulator for field assessment of splash and slope wash in remote locations. Earth Surf. Process. Landforms 32, 2052–2069.

Eltz, F.L.F., Norton, L.D., 1997. Surface roughness as affected by rainfall erosivity, tillage, and canopy cover. Soil Sci. Soc. Am. J. 61, 1746–1755.

Erpul, G., Gabriels, D., Janssens, D., 1998. Assessing the drop size distribution of simulated rainfall in a wind tunnel. Soil Tillage Res. 3–4, 455–463.

Esteves, M., Planchon, O., Lapetite, J.M., Silveira, N., Cadet, P., 2000. The "Empire" large rainfall simulator: design and field testing. Earth Surf. Process. Landforms 25, 681–690.

FAO, 1988. Revised Legend of the FAO_UNESCO Soil Map of the World. World Soils Resources Report, No. 60.FAO/UNESCO/ISRIC, Rome.

FAO, 1993. Soil tillage in Africa: needs and challenges. FAO Soils Bulletin 69, Rome.

Fleskens, L., Stroosnijder, L., Ouessar, M., De Graaff, J., 2005. Evaluation of the on-site impact of water harvesting in southern Tunisia. J. Arid. Environ. 62, 613–630.

Foster, G.R., Meyer, L.D., 1975. Mathematical simulation of upland erosion by fundamental erosion mechanics. Present and Prospective Technology for Predicting Sediment Yields and Sources, Proceedings of the Sediment-Yield Workshop. USDA Sediment Lab, Oxford, Miss. USA, p. 285.

Foster, I.D.L., Fullen, M.A., Brandsma, R.T., Chapman, A.S., 2000. Drip-screen rainfall simulators for hydro and pedo-geomorphological research: the Coventry experience. Earth Surf. Process. Landforms 25 (7), 691–707.

Gao, X., Wu, P., Zhao, X., Wang, J., Shi, Y., 2013. Effect of land use on soil moisture variations in semi-arid catchment: implication for land and agricultural water management. Land Degrad. Dev. http://dx.doi.org/10.1002/ldr.1156.

Hackwell, S.G., Rochester, E.W., Yoo, K.H., Burt, E.C., Monroe, G.E., 1991. Impact of reservoir tillage on water intake and soil erosion. Trans. ASAE 34, 436–442.

Hall, M.J., 1970. Use of stain method in determining the drop-size distributions of coarse liquid sprays. Trans. ASAE 13, 33–41.

Humphry, J.B., Daniel, T.C., Edwards, D.R., Sharpley, A.N., 2002. A portable rainfall simulator for plot-scale runoff studies. Appl. Eng. Agric. 18, 199–204.

Jordán, A., Zavala, L.M., Juan, G., 2010. Effects of mulching on soil physical properties and runoff under semi-arid conditions in southern Spain. Catena 81, 77–85.

Kakembo, V., Ndlela, S., Cammeraat, E., 2013. Trends in vegetation patchiness loss and implication for landscape function: the case of Pteronia Incana Invasion in the Eastern Cape Province, South Africa. Land Degrad. Dev. 23 (6), 548–556. http://dx.doi.org/10.1002/ldr.2175 (November/December 2012).

Kronen, M., 1994. Water harvesting and conservation techniques for small-holder crop production. Soil Tillage Res. 32, 71–86.

Lal, R., 1999. Soil Quality and Soil Erosion. Soil and Water Conservation Society, Boca Raton, FL.

Lascano, R.J., Vorheis, J.T., Baumhardt, R.L., Salisbury, D.R., 1997. Computer controlled variable intensity rain simulator. Soil Sci. Soc. Am. J. 61, 1182–1189.

Martínez-Mena, F., Abadía, R., Castillo, V., Albadalejo, J., 2001. Diseñño experimental mediante lluvia simulada para el estudio de los cambios en la erosión del suelo durante la tormenta. Cuaternario y Geomorfología. 15, 31–43.

Miller, W.P., 1987. A solenoid-operated, variable intensity rainfall simulator. Soil Sci. Soc. Am. J. 51, 832–834.

Mrabet, R., 2002. Stratification of soil and organic matter under tillage systems in Africa. Soil Tillage Res. 66, 119–128.

Munster, C.L., Taucer, P.I., Wilcox, B.P., Porter, S.C., Richards, C.E., 2006. An approach for simulating rainfall above the tree canopy at the hillslope scale. Trans. ASABE 49, 915–924.

Navas, A., Alberto, F., Machín, J., Galán, A., 1990. Design and operation of a rainfall simulator for field studies on runoff and soil erosion. Soil Technol. 3, 385–397.

Niebes, D., Schobel, S., Schneider, R., Schróder, D., 2001. Sprinkling experiments to characterize the influence of land coverage, land use and different soil types on runoff generation. Geophysical Research Abstracts 3.

Oweis, T., Hachum, A., 2006. Water harvesting and supplemental irrigation for improved water productivity of dry farming systems in West Asia and North Africa. Agric. Water Manage. 80, 57–73.

Patrick, C., 2005. Reservoir Tillage for Semi-arid Environments. (PhD thesis) Cranfield University, Silsoe.

Patrick, C., Kechavarzi, C., James, I.T., Dogherty, M.O., Godwin, R.J., 2007. Developing reservoir tillage technology for semi-arid environments. Soil Use Manag. 23, 185–191.

Pérez-Latorre, F.J., de Castro, L., Delgado, A., 2010. A comparison of two variable intensity rainfall simulators for runoff studies. Soil Tillage Res. 107, 11–16.

Ries, J.B., Seeger, M., Iserloh, T., Wistorf, S., Fister, W., 2009. Calibration of simulated rainfall characteristics for the study of soil erosion on agricultural land. Soil Tillage Res. 106, 109–116.

Rochester, E.W., Hill, D.T., Yoo, K.H., 1994. Impact of reservoir tillage on run-off quality and quantity. Trans. ASABE 37 (4), 1183–1186.

Stott, D.E., Mohtar, R.H., Steinhardt, G.C., 2001. Water Conservation, Harvesting and Management (WCHM) — Kenyan Experience.

Ventura, E., Norton, L.D., Ward, K., López-Bautista, M., Tapia-Naranjo, A., 2005. A new reservoir tillage system for crop production in semiarid areas. ASAE Annual Meeting. ASABE (http://asae.frymulti.com/request.asp? Accessed 18 December).

Wiesner, J., 1895. Beitrage zur Kenntnis der tropischen Regens. Math. Naturwiss. Klasse Akad. Wiss. 104, 1397–1434.